

# Bifurcation analysis of a photoreceptor interaction model for Retinitis Pigmentosa



Erika T. Camacho<sup>a,\*</sup>, Anca Radulescu<sup>b</sup>, Stephen Wirkus<sup>a</sup>

<sup>a</sup>School of Mathematical and Natural Sciences, Arizona State University, 4701 W. Thunderbird Rd, Glendale, AZ 85306, USA

<sup>b</sup>Department of Mathematics, SUNY - New Paltz, 1 Hawk Drive, New Paltz, NY 12561, USA

## ARTICLE INFO

### Article history:

Received 30 September 2015

Revised 19 January 2016

Accepted 28 February 2016

Available online 4 March 2016

### Keywords:

Photoreceptor degeneration

Bifurcation

## ABSTRACT

Retinitis Pigmentosa (RP) is the term used to describe a diverse set of degenerative eye diseases affecting the photoreceptors (rods and cones) in the retina. This work builds on an existing mathematical model of RP that focused on the interaction of the rods and cones. We non-dimensionalize the model and examine the stability of the equilibria. We then numerically investigate other stable modes that are present in the system for various parameter values and relate these modes to the original problem. Our results show that stable modes exist for a wider range of parameter values than the stability of the equilibrium solutions alone, suggesting that additional approaches to preventing cone death may exist.

© 2016 Elsevier B.V. All rights reserved.

## 1. Introduction

Retinitis Pigmentosa (RP) is an inherited disease affecting both the rod photoreceptors and cone photoreceptors in the retina. Particularly puzzling to researchers is that all manifestations of RP are caused by mutations in the rods, which cause them to die first, yet cone death always follows [12,13,23–25]. The cones are necessary for daylight vision and acuity while the rods are responsible for night vision. Thus it is crucial to find a way to stop the demise of the cones. Unfortunately, patients typically come to the doctor and are diagnosed with RP once their daylight vision is beginning to be lost, which is often far into the disease progression. While numerous therapies exist that can slow the progression of RP, there is no cure for it [9,10,12,13,15,23,24,26,28].

The photoreceptors (rods and cones) are the most metabolically active cells in the body. Each rod and cone is made up of outer segment (OS) discs that receive and process the light that falls on the retina. There are about 1000 OS discs present in each rod and cone cell and each cell undergoes daily periodic shedding of about 10% of these spent discs. To offset these shed discs, there is a continual renewal of them occurring with the height of the photoreceptor remaining approximately constant [2,11,14,20,29–31]. Once a rod or cone dies, it cannot regenerate itself [21,22]. However, the shedding and renewal of the OS discs support the interpretation of birth and death of photoreceptors for the mathematical model in this manuscript as well as fractions of photoreceptors.

The process of renewal of the discs involves nutrients, glucose, and other trophic factors, most of which pass through the retinal pigment epithelium (RPE) as it is supplied to the photoreceptors [4,5,18,19]. We do not distinguish between any of these and consider them collectively as nutrients. Previous work proposed and detailed this mathematical model, including a

\* Corresponding author. Tel.: +1 602 543 8156; fax: +1 602 543 6073.

E-mail addresses: [erika.camacho@asu.edu](mailto:erika.camacho@asu.edu) (E.T. Camacho), [radulesa@newpaltz.edu](mailto:radulesa@newpaltz.edu) (A. Radulescu), [swirkus@asu.edu](mailto:swirkus@asu.edu) (S. Wirkus).

discussion of the parameter values obtained from data and examining the inverse problem [3,8]. The mathematical analysis focused on the stability of the equilibrium solutions of the model. These solutions predict how a patient suffering from RP can go from a state in which all the photoreceptors are alive to one of complete blindness through different pathways (in parameter space). With numerous different disease progressions experimentally observed in RP patients as well as the various animal models of the disease, the model predictions of various mathematical pathways to blindness is consistent with this.

More specifically, the previous analysis examined stability of equilibrium solutions and saw the progression of the disease represented mathematically as a series of transcritical bifurcations leading to blindness as certain key parameters changed [8]. For a given set of parameter values, it appeared that exactly one stable equilibrium solution existed based on numerical evidence. However, stable limit cycles were observed in certain parameter ranges in this 3- and 4-dimensional phase space. As it is crucial to prevent the loss of the photoreceptors since their complete death results in blindness, we focus our efforts in this paper on the presence of stable limit cycles and the co-existence of multiple stable modes. These stable limit cycles have the physiological interpretation of periodically varying levels of OS discs, which could result from the rhythmic shedding and renewal of the OS discs if their period is near 24 h or some other type of stable behavior even if the period is not near 24 h. Thus, even if no stable equilibrium point exists, the presence of a stable limit cycle or other stable attracting structure could give insight into mechanisms and parameters in which experimental researchers could focus their efforts in attempting to slow or stop the disease. Current experimental research is focusing on ways to increase the supply of glucose and nutrient uptake into the cell [1,27]. Our work ties into this as it may suggest other areas of parameter space in which experimentalists could explore.

This paper examines dynamic behavior (Hopf bifurcations, fold bifurcations, etc.) in realistic parameter ranges and we find this same type of behavior in a wider parameter range, although not as realistic. Our extensive numerical investigation gives confirmation that the same qualitative behavior is observed for both realistic parameter ranges and less-realistic parameter ranges. However, the narrowness of realistic parameter ranges makes it difficult to visualize all the rich behavior of the system. Thus for the purpose of visualization we will focus on the larger (less-realistic) parameter range for this article.

**2. Mathematical model**

The work of Camacho et al. [6] and Camacho and Wirkus [8] considers a mathematical model of photoreceptor interactions:

$$\begin{aligned} \dot{R}_n(t) &= R_n(a_n T - \mu_n - m), \\ \dot{R}_m(t) &= R_m(a_m T - \mu_m) + m R_n, \\ \dot{C}(t) &= C(a_c T - \mu_c + d_n R_n + d_m R_m), \\ \dot{T}(t) &= T(\Gamma - kT - \beta_n R_n - \beta_m R_m - \gamma C), \end{aligned} \tag{1}$$

where all variables are functions of  $t$  and

$R_n$  = number of outer segments of normal rods,

$R_m$  = number of outer segments of “sick” rods,

$C$  = number of outer segments of cones,

$T$  = number of RPE cells (trophic pool for  $R_n, R_m, C$ ),

$\mu_i$  = shedding (energy consumption) rates of  $R_n, R_m, C$  (units = 1/day),

$m$  = rate at which rods phenotypically express mutation and rod functionality is compromised (i.e., become “sick”),

$d_n, d_m$  = direct help of RdCVF (Rod-derived Cone Viability Factor) given to cones by rods (units = 1/(day · rod OS)), [7,16,17],

$\beta_n, \beta_m, \gamma$  = rate of trophic pool usage by photoreceptors (units = 1/(day · OS)),

$a_i$  = renewal (energy uptake) rate of trophic pool into new outer segments (proportional to  $\beta_i, \gamma$ ; units = 1/(day · RPE)),

$\frac{\Gamma}{k}$  = carrying capacity of trophic pool in absence of photoreceptors (units = RPE).

The realistic ranges of the various parameters and variables are orders of magnitude apart. For example, the contribution of RdCVF from the rods is estimated to be  $d \approx 1 \times 10^{-11}$ , the shedding rates  $\mu_i \approx 0.1$ , and the rod population  $R(0) \approx 1 \times 10^8$  [8]. Thus, we nondimensionalize the system with the substitutions

$$\begin{aligned} x &= \frac{R_n d_n}{\mu_c}, \quad w = \frac{R_m d_n}{\mu_c}, \quad y = \frac{C \gamma}{\Gamma}, \quad z = \frac{T a_n}{\mu_n}, \\ b_1 &= \frac{a_c \mu_n}{\mu_c a_n}, \quad b_2 = \frac{\beta_n \mu_c}{\Gamma d_n}, \quad b_3 = \frac{k \mu_n}{\Gamma a_n}, \quad b_4 = \frac{a_m \mu_n}{\mu_m a_n}, \\ b_5 &= \frac{d_m}{d_n}, \quad b_6 = \frac{\beta_m \mu_c}{\Gamma d_n}, \quad M = \frac{m}{\Gamma}, \quad \tau = \frac{t}{\Gamma}, \\ \gamma_1 &= \frac{\mu_n}{\Gamma}, \quad \gamma_2 = \frac{\mu_c}{\Gamma}, \quad \gamma_3 = \frac{\mu_m}{\Gamma} \end{aligned} \tag{2}$$

and obtain the dimensionless equations

$$x' = \gamma_1 x(z - 1) - Mx,$$

$$\begin{aligned}
 w' &= \gamma_3 w(b_4 z - 1) + Mx, \\
 y' &= \gamma_2 y(b_1 z - 1 + x + b_5 w), \\
 z' &= z(1 - b_3 z - b_2 x - b_6 w - y),
 \end{aligned}
 \tag{3}$$

where the derivatives are now with respect to rescaled time  $\tau$ . This is the system that we analyze in this current paper. While it is equivalent to System (1), the rescaling allows for more stable numerical methods and for the solutions to be obtained much more quickly than with the original system because the parameters and variables are now near the same orders of magnitude. The equilibria of System (1) and their stability have been examined in [8]; however, only transcritical bifurcations were presented. As we will see in the ensuing discussion, the rescaled system does have stable periodic motions and we use bifurcation theory to determine their origin. Additionally, for the purposes of interpretation of the physiological meaning of some of our solutions, we introduce 4 key ratios (each of which is dimensional):

$$D_T = \frac{\Gamma}{k}, \quad D_m = \frac{\mu_m}{a_m}, \quad D_c = \frac{\mu_c}{a_c}, \quad D_n = \frac{\mu_n + m}{a_n}.
 \tag{4}$$

The first of these ratios,  $D_T$ , can be interpreted as the carrying capacity of the nutrient flow into the system in the absence of photoreceptors. The next two ratios,  $D_m$  and  $D_c$ , can be interpreted as the ratio of the energy consumption to energy uptake of the photoreceptors for the sick rods and cones, respectively. The final ratio,  $D_n$ , is a modification of the energy consumption to uptake ratio of the healthy rods that includes the exiting from this class of healthy rods. In examining the existence and stability of the equilibria, we will see that the difference of these ratios will be crucial in interpreting the solutions.

### Equilibria

There are seven equilibrium solutions  $(x, w, y, z)$ :

$$\begin{aligned}
 E_1 &= (0, 0, 0, 0); \quad E_2 = \left(0, 0, 0, \frac{1}{b_3}\right); \quad E_3 = \left(0, \frac{b_4 - b_3}{b_4 b_6}, 0, \frac{1}{b_4}\right); \\
 E_4 &= \left(0, 0, \frac{b_1 - b_3}{b_1}, \frac{1}{b_1}\right); \quad E_5 = \left(0, \frac{b_4 - b_1}{b_4 b_5}, \frac{b_5(b_4 - b_3) - b_6(b_4 - b_1)}{b_4 b_5}, \frac{1}{b_4}\right); \\
 E_6 &= (x^*, w^*, y^*, z^*), \quad \text{with} \\
 z^* &= \frac{\gamma_1 + M}{\gamma_1}, \quad y^* = 0, \quad x^* = \frac{\gamma_3(b_3 z^* - 1)(b_4 z^* - 1)}{b_6 M - \gamma_3 b_2(b_4 z^* - 1)}, \quad w^* = \frac{1 - b_3 w^* - b_2 x^*}{b_6}; \\
 E_7 &= (x_*, w_*, y_*, z_*), \quad \text{with} \\
 z_* &= \frac{\gamma_1 + M}{\gamma_1}, \quad w_* = \frac{M(b_1 z_* - 1)}{\gamma_3(b_4 z_* - 1) - b_5 M}, \quad x_* = 1 - b_1 z_* - b_5 w_*, \quad y_* = 1 - b_3 z_* - b_2 x_* - b_6 w_*.
 \end{aligned}$$

As the cones are completely responsible for day vision, we are most interested in the solutions  $E_4, E_5$ , and  $E_7$  in which the cone population still exists. In the disease RP, the typical progression to blindness in RP is given by  $E_7 \rightarrow E_5 \rightarrow E_4 \rightarrow E_2$  and numerous paths in parameter space can be found that give this progression [8,24].

### Stability

While we are most concerned with equilibria  $E_4, E_5$ , and  $E_7$  as these equilibria correspond with daylight vision, we will still consider each equilibrium as their locations and their eigenvalues demonstrate the series of transcritical bifurcations that correspond to the progression to blindness observed in RP. It will also allow us to see potential coexistence of stable modes. The Jacobian of the system is

$$J = \begin{pmatrix} \gamma_1(z-1) - M & 0 & 0 & \gamma_1 x \\ M & \gamma_3(b_4 z - 1) & 0 & \gamma_3 b_4 w \\ \gamma_2 y & \gamma_2 b_5 y & \gamma_2(b_1 z - 1 + x + b_5 w) & \gamma_2 b_1 y \\ -b_2 z & -b_6 z & -z & 1 - b_2 x - b_6 w - y - 2b_3 z \end{pmatrix}.$$

The eigenvalues for  $E_1$  are easily seen to be  $1, -\gamma_2, -\gamma_3, -(\gamma_1 + M)$ . Hence  $E_1$  is always a saddle. Equilibrium  $E_2$  always exists physiologically and corresponds to complete blindness and is the final stage in RP. The eigenvalues of  $E_2$  are easily seen to be  $-1, \frac{\gamma_2(b_1 - b_3)}{b_3}, \frac{\gamma_3(b_4 - b_3)}{b_3}, \frac{\gamma_1(1 - b_3)}{b_3} - M$ . In terms of our key physiological ratios, it is stable when  $D_T < \min\{D_n, D_m, D_c\}$ . Thus, if the nutrient supply is small enough, all photoreceptors will die.

The eigenvalues of  $E_3$  are seen to be

$$\lambda_1 = \gamma_1 \left(\frac{1}{b_4} - 1\right) - M, \quad \lambda_2 = \gamma_2 \left(\frac{b_1}{b_4} - 1 + \frac{b_5(b_4 - b_3)}{b_4 b_6}\right), \quad \lambda_{3,4} = \frac{-b_3 \pm \sqrt{b_3^2 - 4b_4 \gamma_3(b_4 - b_3)}}{2b_4}.$$

While there are parameter values for which this solution can be stable and physiologically relevant, this state corresponds to no cones and occurs in the far-less common reverse RP [12,13,25]. Equilibrium  $E_4$  is the final state in which cones exist and is physiologically relevant when  $D_T > D_c$ , i.e., when the nutrient supply is sufficiently large compared to the consumption to uptake ratio of the cones. Its eigenvalues are seen to be

$$\lambda_1 = \gamma_1 \left( \frac{1}{b_1} - 1 \right) - M, \quad \lambda_2 = \frac{\gamma_3(b_4 - b_1)}{b_1}, \quad \lambda_{3,4} = \frac{-b_3 \pm \sqrt{b_3^2 - 4b_4\gamma_2 b_1(b_1 - b_3)}}{2b_1}.$$

We can again interpret the stability in terms of our key ratios.  $E_4$  will be stable when  $D_c < \min\{D_T, D_n, D_m\}$ , which suggests that the consumption to uptake ratio of the cones needs to be smaller than that of both types of rods together with a sufficient nutrient supply. Thus there is a region in parameter space for which this solution is stable and physiologically relevant. This also suggests that the demise of the rods and concurrent survival of the cones can be interpreted as either a change in  $D_c$  or a change in both  $D_n, D_m$  for a fixed  $D_T$  to satisfy the inequalities or, alternatively, a change in  $D_T$  for the other parameters fixed.

Another state of crucial interest is  $E_5$  in which some rods and most cones remain. As mentioned earlier, patients typically do not report problems to the doctor regarding difficulty seeing at night but rather report problems with daylight vision (once cones have begun to degenerate) [12,13,25]. Thus while it is best to theoretically focus on  $E_7$ , which would represent a case of early detection, understanding  $E_5$  represents the more realistic scenario. One eigenvalue of  $E_5$  is given by  $\lambda_1 = \gamma_1(\frac{1}{b_4} - 1) - M$ , and the three others are given by the equation:

$$\lambda^3 - A\lambda^2 + \lambda \left[ \frac{\gamma_3 b_6(b_4 - b_1)}{b_4 b_5} + \frac{\gamma_2 b_1 K}{b_4^2 b_5} \right] + \frac{\gamma_2 \gamma_3 K(b_4 - b_1)}{b_4^2 b_5} = 0, \tag{5}$$

where  $K = b_5(b_4 - b_3) - b_6(b_4 - b_1)$ , and  $A = 1 - \frac{b_6(b_4 - b_1)}{b_4 b_5} - \frac{K}{b_4 b_5} - \frac{2b_3}{b_4}$ . Explicit solutions for this are complicated, but the  $\lambda = 0$  bifurcations are given by

$$\frac{\gamma_2 \gamma_3 (b_4(\gamma_1 + M) - \gamma_1)(b_4 - b_1)(b_5(b_4 - b_3) - b_6(b_4 - b_1))}{b_5 b_4^2} = 0.$$

It is also straightforward to check whether this equilibrium could go through a Hopf bifurcation for any parameter values. At a Hopf parameter point, two eigenvalues have to be complex numbers, so that the equation above would be of the form

$$(\lambda - a)(\lambda^2 + \tau^2) = \lambda^3 - a\lambda^2 + \tau^2\lambda - a\tau^2 = 0.$$

Comparing the previous equation with (5) gives  $a = A$  and  $\tau^2 = \frac{\gamma_3 b_6(b_4 - b_1)}{b_4 b_5} + \frac{\gamma_2 b_1 K}{b_4^2 b_5}$ , thus leading to the following two conditions:

$$\frac{\gamma_3 b_6(b_4 - b_1)}{b_4 b_5} + \frac{\gamma_2 b_1 K}{b_4^2 b_5} > 0 \text{ and } A \left[ \frac{\gamma_3 b_6(b_4 - b_1)}{b_4 b_5} + \frac{\gamma_2 b_1 K}{b_4^2 b_5} \right] + \frac{\gamma_2 \gamma_3 K(b_4 - b_1)}{b_4^2 b_5} = 0. \tag{6}$$

These conditions are satisfied in many circumstances. For example, one may fix all parameters except  $b_1$ , and study the system’s sensitivity to changes in  $b_1$ . Since  $K$  depends linearly on  $b_1$ , there could be as many as two Hopf points along the curve  $E_5(b_1)$ .

For the equilibria  $E_6$ , one eigenvalue is  $\lambda_3 = \frac{\gamma_2 \gamma_3 (b_4(\gamma_1 + M) - \gamma_1) - b_5 M \gamma_1}{b_2 \gamma_3 (b_4(\gamma_1 + M) - \gamma_1) - b_6 M \gamma_1}$ . The  $\lambda = 0$  bifurcations are given by

$$\frac{(\gamma_1 + M)(b_4(\gamma_1 + M) - \gamma_1)(b_3(\gamma_1 + M) - \gamma_1)\gamma_3}{\gamma_1^2} = 0.$$

As with  $E_3$ , we do not focus on  $E_6$  since it is a state in which cones have already degenerated.

For the equilibria  $E_7$ , the stability is more difficult to establish analytically as the eigenvalues are given by a complicated fourth order polynomial. The  $\lambda = 0$  bifurcations are given by

$$\frac{\gamma_2 \gamma_3 (\gamma_1 + M)(b_4(\gamma_1 + M) - \gamma_1)(b_1(\gamma_1 + M) - \gamma_1)}{\gamma_1^2} = 0.$$

It is easy to illustrate, however, that  $E_7$  is likely to undergo interesting bifurcations when one or two parameters are varied.

### 3. Numerical results

Previous work has suggested that no more than one equilibrium point is stable for a given set of parameter values and that changing the parameters can lead to a sequence of transcritical bifurcations that corresponds to the progression of the disease [8]. However, we have observed stable limit cycles in the model in both 3- and 4-dimensional phase space and want to examine the possible co-existence of various stable modes. These stable modes have the physiological interpretation of periodically varying levels of OS discs, which could result from the rhythmic shedding and renewal of the OS discs. As mentioned earlier, as of yet there is no therapy that can stop the progression of RP [12,13,16,23–25]. Thus gaining a better understanding of the stable solutions that exist for various parameters can suggest to researchers what parameter ranges may be targeted or desired. We will focus on the equilibria  $E_5$  and  $E_7$  in which both cones and some rods still exist and explore other stable modes with MatCont.

### 3.1. Large parameters

We will investigate numerically the local behavior of the system in a parameter range based at  $b_2 = \frac{5}{4}$ ,  $b_3 = \frac{2}{21}$ ,  $b_4 = \frac{513}{560}$ ,  $b_5 = \frac{55}{2}$ ,  $b_6 = \frac{5}{4}$ ,  $M = \frac{1}{150}$ ,  $\gamma_1 = \frac{4}{15}$ ,  $\gamma_2 = \frac{1}{60}$ ,  $\gamma_3 = \frac{4}{15}$ , where for certain  $b_1$ -values a stable limit cycle has been observed. If  $b_1$  is allowed to change, one can compute the Hopf points along the curve  $E_5(b_1)$  to be at  $b_1 \sim -12.9566$  and at  $b_1 = 0.5817$ . We want to illustrate the behavior at the Hopf bifurcation points, and observe the evolution and stability-changing bifurcations of the limit cycles that resulted at the Hopf point. To do this, we used the MatCont package, as follows.

Start, for example, at  $b_1 = 0.8$ , where it can be checked that equilibrium  $E_5 = (0, 0.0046, 0.8903, 1.0916)$  is stable. Then the equilibrium curve for  $E_5$ , tracked as  $b_1$  changes, runs into Branch Points at  $b_1 = 0.91$  and  $b_1 = -17.14$ , Neutral Saddles at  $b_1 = 1.12$  and  $b_1 = -19.95$ , and into two supercritical Hopf points, as expected, at  $b_1 \sim 0.58$  and  $b_1 = -12.95$ .

For each Hopf point, we extend the cycle with respect to  $b_1$  (and the Period), while monitoring singularities. The evolution of the cycles is illustrated in a  $(w, y)$  slice of the phase space in Fig. 1 (using integration parameters:  $ntst = 50$ ,  $ncol = 4$ ,  $InitStepsize = 1$ ,  $MinStepsize = 0.1$ ,  $MaxStepsize = 5$   $Adapt = 3$ ). Bifurcation diagrams for the two Hopf points are shown in Fig. 2 (using integration parameters:  $ntst = 50$ ,  $ncol = 4$ ,  $InitStepsize = 0.5$ ,  $MinStepsize = 0.1$ ,  $MaxStepsize = 1$ ,  $Adapt = 30$ ). Further local bifurcations of the cycles are illustrated in Figs. 1 and 2. For example, the cycle sprouting out of the positive Hopf point undergoes two fold bifurcations, one at  $b_1 \sim 0.4161$  and one at  $b_1 \sim 0.4282$ , so that in the small window between these two values, the system has multistability: an unstable equilibrium and three cycles (two of which are stable).

We can further track down the Hopf point when changing another parameter simultaneously with  $b_1$  (e.g.,  $b_3$ , for Fig. 3). On one side of the Hopf curve from Fig. 3 we have an attracting equilibrium (i.e., for the initial conditions in its basin of attraction, solutions converge asymptotically to an attracting point); on the other side of the curve, the convergence is to a stable limit cycle (i.e., the system starting with the same initial conditions will go into sustained oscillations). The parameter values at each of these bifurcations give  $E_7$  as stable and  $E_5$  as unstable with both physiologically relevant. Thus, the stable limit cycle represents a potential stable mode that could be present in an early stage of RP.

We now illustrate a series of phenomena for the equilibrium  $E_7$ . At the same initial parameters as at the start of this section,  $E_7$  is stable and can be calculated:  $E_7 = (0.0147, 0.006, 0.8765, 1.025)$ . Integrating backwards with respect to  $b_4$ , one finds a supercritical Hopf bifurcation at  $b_4 \sim 1.04418$ . Extending the stable cycle, we run into other local bifurcations (Neutral Saddle, Period Doubling and Limit Point Cycles (as shown in Fig. 4)). Equating mathematically stable modes with physiologically relevant possibilities of photoreceptor life suggests that identifying RP early in a patient may be crucial to helping prolong the life of the photoreceptor since the stable modes were born from  $E_7$ .

### 3.2. Small parameters

Still within reasonable parameter ranges, we now investigate numerically the local behavior of the system with parameters  $b_1 = 1.5$ ,  $b_2 = 5.8$ ,  $b_3 = 0.79$ ,  $b_4 = 0.8$ ,  $b_5 = 1$ ,  $b_6 = 5.8$ ,  $\gamma_1 = 0.071$ ,  $\gamma_2 = 0.075$ ,  $\gamma_3 = 0.071$ ,  $M = 2.4 \cdot 10^{-7}$ . For this set of parameters, we can calculate the equilibrium  $E_5 = (0, -0.875, 5.0875, 1.25)$ .

We initiate the equilibrium at this point, and compute backward for the parameter  $b_3$ , with the default setup. The algorithm will run into a supercritical Hopf point at  $b_3 \sim -0.04554$  (with very small, but still negative Lyapunov coefficient). We extend the stable cycle (locally) from the Hopf point, with amplitude = 0.1,  $ntst = 60$ ,  $ncol = 4$ ,  $InitStepsize = 0.1$ ,  $MinStepsize = 0.1$ , and  $MaxStepsize = 5$  (or smaller, for a more opaque diagram). This evolution is shown in the phase space  $(y, z)$  in Fig. 5(a), and as a bifurcation diagram with respect to the parameter  $b_3$  in Fig. 5(b).

We return to the original equilibrium, and compute backward for the parameter  $b_6$ , with the default setup. The algorithm will run into a Hopf point at  $b_6 \sim -0.0275$ . We extend the cycle from the Hopf point, with amplitude = 0.01,  $ntst = 60$ ,  $ncol = 4$ ,  $InitStepsize = 0.1$ ,  $MinStepsize = 0.1$ , and  $MaxStepsize = 5$ . This runs into a limit point cycle around  $b_6 \sim -0.0282$ . The cycle evolution is shown in the phase space  $(z, w)$  in Fig. 6(a), and as a bifurcation diagram in Fig. 6(b).

The evolution of the Hopf bifurcation as both parameters  $b_3$  and  $b_6$  change simultaneously is shown in Fig. 7(a) and (b). We illustrate this as a Hopf curve, on which we mark the codimension 2 bifurcations: the Bogdanov–Takens point (BT, purple) occurs at  $(b_3, b_6) \sim (0.8, 0)$ ; the Neutral Saddle (HH) point (HH, orange)  $(b_3, b_6) \sim (0.014, -1.362)$ ; the Zero Hopf point (ZH, brown) occurs at  $(b_3, b_6) \sim (0, -1.142)$ ; the Generalized Hopf (GH, red) occurs at  $(b_3, b_6) \sim (-0.029, 0.322)$ . The figure also presents the bifurcation diagram showing the  $z$ -coordinate of the Hopf point with respect to  $b_3$  and the same Hopf curve represented in the  $(b_3, b_6)$  parameter plane.

This is a range more compatible with the parameter ranges estimated empirically. Quite interestingly, the windows of bistability created by the fold bifurcations (in which a stable equilibrium coexists with a stable cycle) are extremely small, so that bistable behavior requires very fine tuning of the parameters.

## 4. Discussion

We have found numerous stable solutions that co-exist with the equilibria  $E_5$  and  $E_7$  in the progression of RP, some of which are physiologically relevant (nonnegative variable-values). These stable solutions have the physiological interpretation of periodically varying levels of OS discs, which could result from the rhythmic shedding and renewal of the OS discs. In particular, the presence of a stable limit cycle from  $E_5$  when  $E_7$  is still stable represents a highly desirable stable mode in

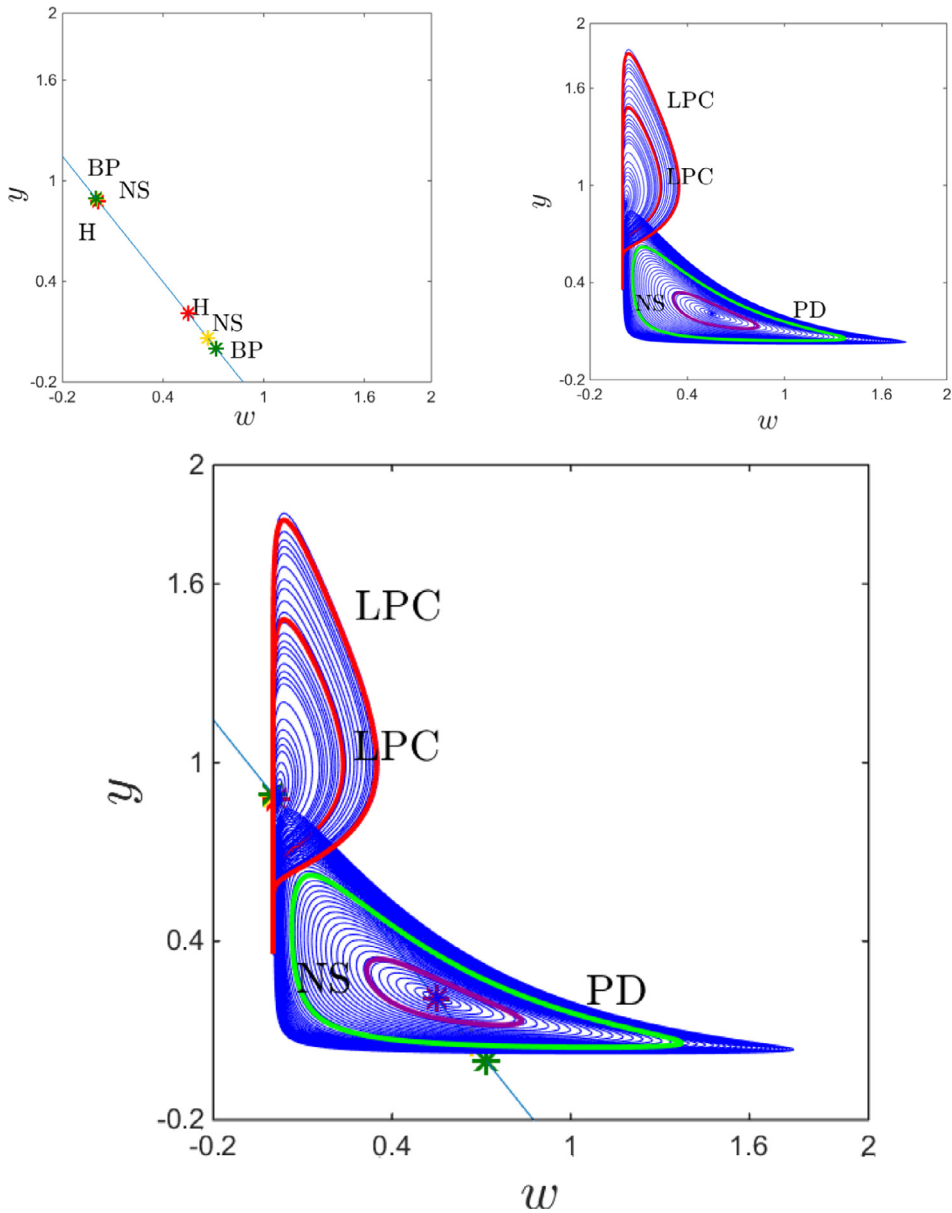


**Fig. 1.** Hopf points (H) and cycles in the phase plane, for the  $E_5$  equilibrium curve with respect to the parameter  $b_1$ . The projection of the equilibrium curve  $E_5(b_1)$  is shown in the  $(w, y)$  phase space slice (top left panel; superimposed in bottom panel). The two Hopf points are shown as red stars, the two branch points (BP) are shown as green stars, and the two neutral saddles are shown as yellow stars. The evolution of the stable cycles created through the Hopf bifurcations is illustrated in the  $(w, y)$  plane (top right panel; superimposed in bottom panel). The stable cycle created at the  $b_1 \sim 0.58$  undergoes two further fold (stability changing) bifurcations (Limit Point Cycle (LPC), red) at  $b_1 \sim 0.4161$  and  $b_1 \sim 0.4282$ , and the stable cycle created at the Hopf point  $b_1 \sim -12.95$  undergoes a Neutral Saddle bifurcation (NS, purple) at  $b_1 \sim -12.5160$  and a Period Doubling bifurcation (PD, green) at  $b_1 \sim -9.9223$ . (For interpretation of the references to color in this figure legend, the reader is referred to the web version of this article.)

the early stage of the disease RP. Comparing with realistic parameter values [8], we observe that all known values are close to their reasonable ranges of a healthy patient or one in a patient in the early or mid-stages of the disease.

As described earlier, in RP it is the rods that die first followed inevitably by the cones. While the mutation is present only in the rods, current experimental research has yet to identify precisely why the cones also die. Some experiments suggest that keeping the supply of glucose and nutrients at high enough levels may help prevent or delay cone death [1,27]. Our results confirm this as the quantity  $D_T$  is seen to play a role in the death of each type of photoreceptor. However, keeping the cones alive could also be a matter of making their uptake of nutrients more efficient and this would involve changes in  $D_c$  or  $b_1$  in the rescaled model. For example, the plots in Fig. 2(b) suggest that experimentalists could also focus on changes in either the uptake or consumption within the cones in order to identify ways to prolong their life.

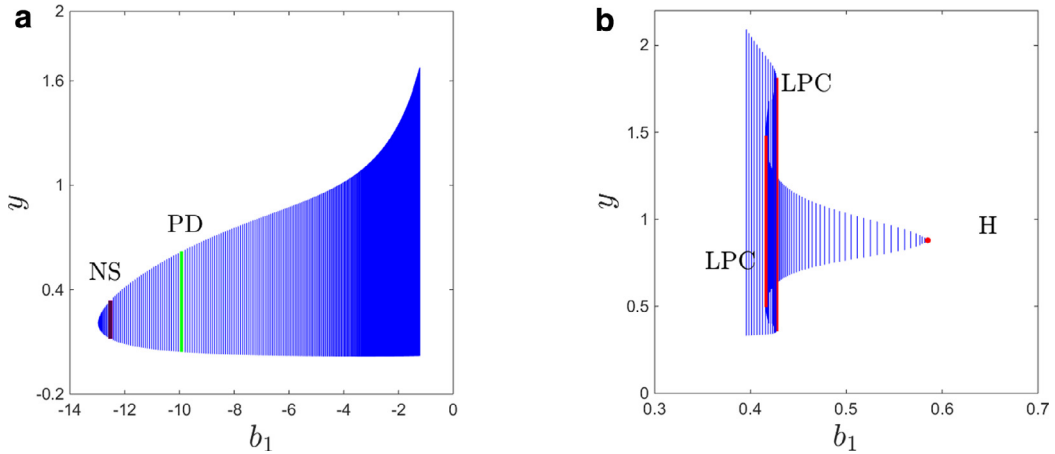


**Fig. 2.** The Hopf bifurcation (H) on  $E_5(b_1)$ , near  $b_1 = 0.58$ . We represent, in the  $y$  cross-section, how the cycle from  $b_1 \sim 0.58$  evolves with respect to the changing parameter  $b_1$ . The red star represents the subcritical Hopf bifurcation, the red vertical segments are the projections of the cycle (LPC) at the two fold points (at  $b_1 = 0.4158$  and  $b_1 \sim 0.426$ ). In the interval of  $b_1$  values between these two folds, three cycles coexist with the equilibrium. Neutral saddle bifurcations (NS) and Period doubling bifurcations (PD) also occur. (For interpretation of the references to color in this figure legend, the reader is referred to the web version of this article.)

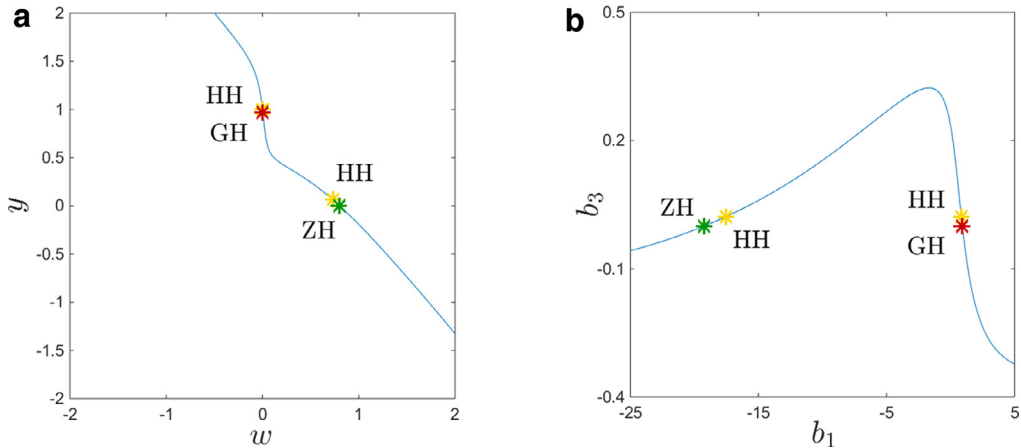


**Fig. 3.** Hopf curve when changing both  $b_1$  and  $b_3$ : (a) in the  $(w, y)$  phase space slice; (b) in the  $(b_1, b_3)$  parameter slice. The stars represent codimension 2 bifurcations: generalized Hopf (GH, red), Zero Hopf (ZH, green) and Neutral Saddles (HH, yellow) (compare with Eq. (6)). (For interpretation of the references to color in this figure legend, the reader is referred to the web version of this article.)

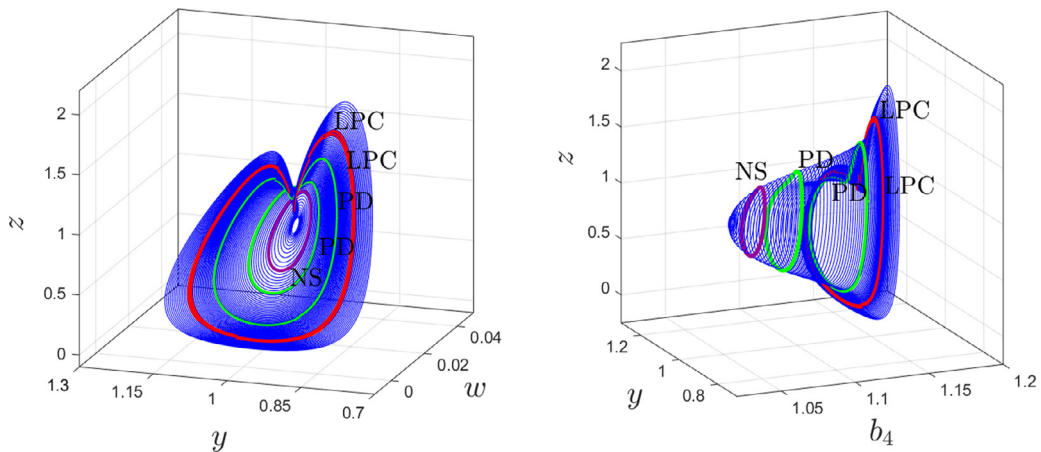


**Fig. 4.** Local bifurcations with respect to  $b_4$  obtained by extending the cycle obtained through the supercritical Hopf bifurcation at  $b_4 \sim 1.0441$  along the equilibrium  $E_7$ . From the Hopf point onwards: Neutral Saddle (NS, purple) at  $b_4 \sim 0.0609$ ; successive Period Doublings (PD, green) at  $b_4 \sim 1.0831$  and  $b_4 \sim 1.1223$ ; successive folds, or Limit Point Cycles (LPC, red) at  $b_4 \sim 1.12912$  and  $b_4 \sim 1.12913$ . (For interpretation of the references to color in this figure legend, the reader is referred to the web version of this article.)

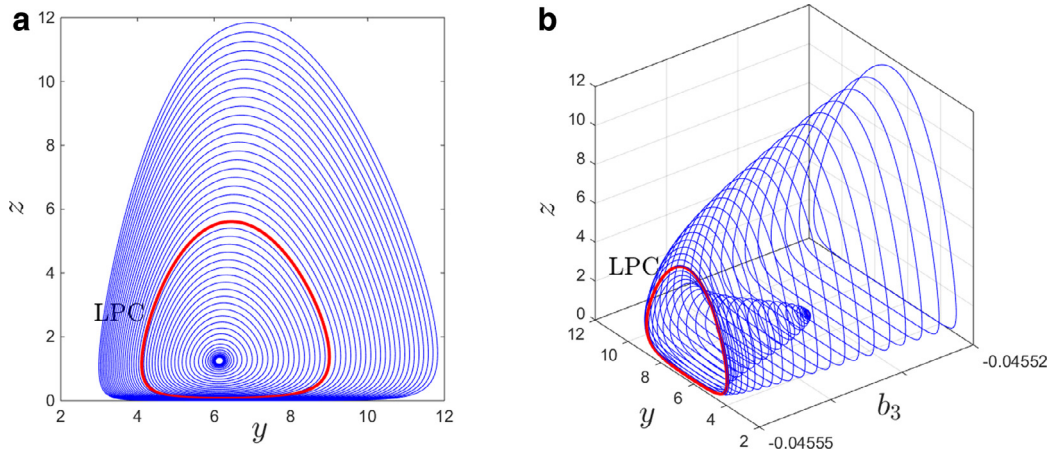


**Fig. 5.** Stable cycle extended out of the Hopf bifurcation at  $b_3 = -0.0455436$ , when  $b_3$  changes. (a) Cycle evolution in a  $(y, z)$  slice of the phase space. (b) Cycle evolution shown as a  $z$ -coordinate versus  $b_3$  bifurcation diagram. The cycle continuation runs into a Limit Point Cycle (or fold) bifurcation (LPC, red curve) at  $b_3 = -0.045549688$ , with the change of the cycle's stability. (For interpretation of the references to color in this figure legend, the reader is referred to the web version of this article.)

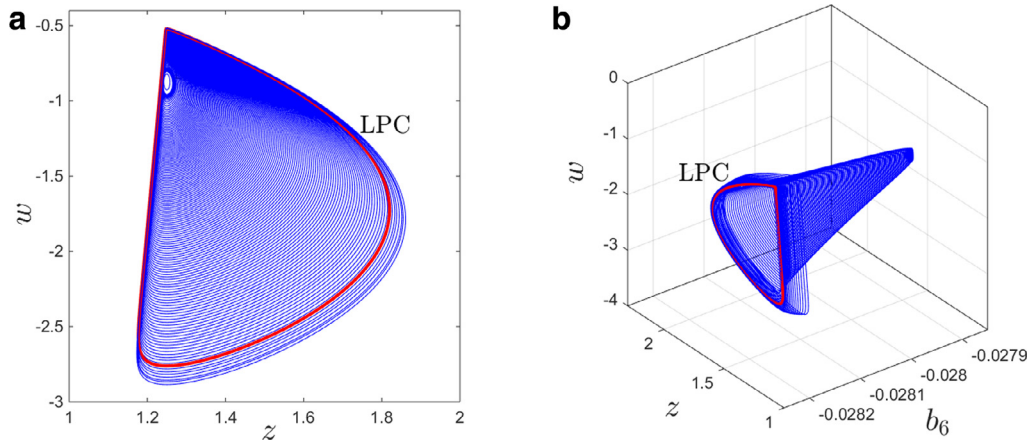


**Fig. 6.** Unstable cycle extended out of the Hopf bifurcation at  $b_6 = -0.027528815$ , when  $b_6$  changes. (a) Cycle evolution in a  $(z, w)$  slice of the phase space. (b) Cycle evolution shown as a bifurcation diagram of the  $(z, w)$  phase space slice versus  $b_6$ . The cycle continuation runs into a Limit Point Cycle bifurcation at  $b_6 = -0.0282$ , with the change in the cycle's stability (LPC, shown in both cases as a red curve). (For interpretation of the references to color in this figure legend, the reader is referred to the web version of this article.)

Our numerical results also identified the existence of alternate stable solutions to  $E_i$  that are present for lower nutrient levels corresponding to the patient being closer to blindness. This further suggests the need to focus on additional parameter ranges to sustain the life of the cones. Additional experiments in which the photoreceptor levels are carefully measured could suggest additional parameter ranges in which the life of the photoreceptors may be prolonged. While we were not able to do so, further work could also examine whether a region of parameter space could be found in which  $E_2$  was the only stable equilibrium point yet a stable limit cycle also existed. This would be of utmost physiological importance as it would suggest that identifying RP in its early stages could avoid permanent blindness. Retinal implants, currently under development and in which photoreceptors are transplanted into an RP retina, could also give initial conditions that would sustain one or more types of photoreceptors even after blindness had occurred.

Our previous work showed the importance of nutrients in preventing the disease from progressing [8]. The smaller  $b_3$ -value corresponds to nutrient levels observed at a more advanced stage of the disease; see Figs. 5 and 7. The parameter  $b_5$  being larger would correspond to an elevated RdCVF contribution from the mutated rods compared with the normal ones; see Fig. 6. No experiments have yet been done to distinguish the levels of RdCVF produced by the two rods, except to say that both produce it. Having a more accurate set of parameter values for these two quantities could help identify desirable parameter ranges that may be achieved.

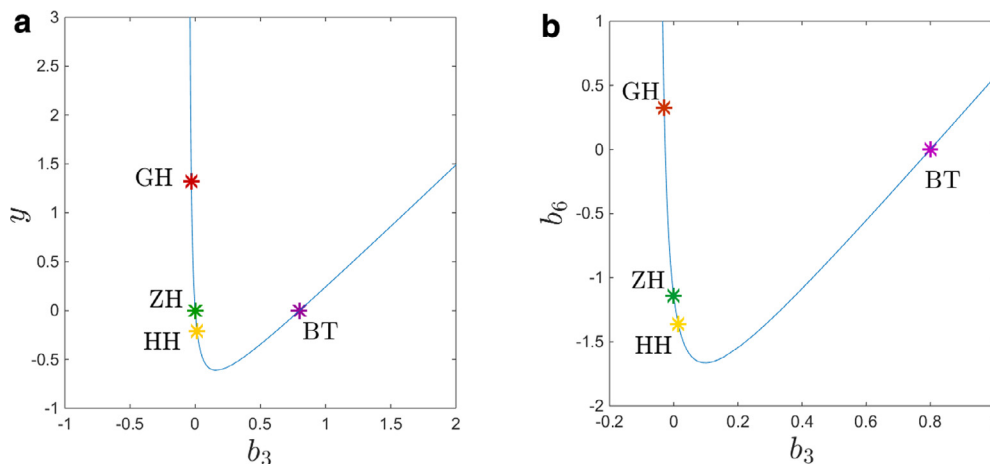


**Fig. 7.** Hopf curve for changing  $b_3$  and  $b_6$ , with codimension two bifurcations marked with colored stars: the Bogdanov–Takens point (BT, purple) occurs at  $(b_3, b_6) \sim (0.8, 0)$ ; the Neutral Saddle (HH) point (HH, yellow)  $(b_3, b_6) \sim (0.014, -1.362)$ ; the Zero Hopf point (ZH, green) occurs at  $(b_3, b_6) \sim (0, -1.142)$ ; the Generalized Hopf (GH, red) occurs at  $(b_3, b_6) \sim (-0.029, 0.322)$ . (a) Bifurcation diagram showing the  $z$ -coordinate of the Hopf point with respect to  $b_3$ . (b) The same Hopf curve represented in the  $(b_3, b_6)$  parameter plane. (For interpretation of the references to color in this figure legend, the reader is referred to the web version of this article.)

## Acknowledgments

We would like to thank the anonymous reviewer for helpful and insightful comments in the revisions of this paper.

## References

- [1] Ait-Ali N, Fridlich R, Millet-Puel G, Clérin E, Delalande F, Jaillard C, et al. Rod-derived cone viability factor promotes cone survival by stimulating aerobic glycolysis. *Cell* 2015;161:817–32.
- [2] Anderson DH, Fisher SK. Disc shedding in rodlike and conelike photoreceptors of tree squirrels. *Science* 1975;187:953–5.
- [3] Banks HT, Davidian M, Samuels Jr JR, Sutton KL. Mathematical and statistical estimation approaches in epidemiology. In: *An Inverse Problem Statistical Methodology Summary*. New York: Springer; 2009. p. 249–302.
- [4] Berson EL. Retinal photoreceptor-pigment epithelium interactions: Friedenwald lecture. *Invest Ophthalmol Vis Sci* 1993;26:1659–94.
- [5] Bok D. Retinal photoreceptor-pigment epithelium interactions: Friedenwald lecture. *Invest Ophthalmol Vis Sci* 1985;26:1659–94.
- [6] Camacho ET, Colón Vélez MA, Hernández DJ, Rodríguez Bernier U, van Laarhoven J, Wirkus S. A mathematical model for photoreceptor interactions. *J Theor Biol* 2010;21:638–46.
- [7] Camacho ET, Melara LA, Villalobos MC, Wirkus SA. Optimal control in the treatment of retinitis pigmentosa. *B Math Biol* 2014;76:292–313.
- [8] Camacho ET, Wirkus S. Tracing the progression of retinitis pigmentosa via photoreceptor interactions. *J Theor Biol* 2013;317C:105–18.
- [9] Cepko C. Effect of gene expression on cone survival in retinitis pigmentosa. *Retina J Retin Vitre Dis* 2005;25(8):S21–4.
- [10] Fain GL, Lisman JE. Photoreceptor degeneration in vitamin A deprivation and retinitis pigmentosa: The equivalent light hypothesis. *Exp Eye Res* 1993;57:335–40.
- [11] Guérin CJ, Lewis GP, Fisher SK, Anderson DH. Recovery of photoreceptor outer segment length and analysis of membrane assembly rates in regenerating primate photoreceptor outer segments. *Invest Ophthalmol Vis Sci* 1993;34:175–83.
- [12] Hamel C. Retinitis pigmentosa. *Orphanet J Rare Dis* 2006;1:40.
- [13] Hartong DT, Berson EL, Dryja TP. Retinitis pigmentosa. *Lancet* 2006;368:1795–809.
- [14] Jonnal RS, Besecker JR, Derby JC, Kocaoglu OP, Cense B, Gao W, et al. Imaging outer segment renewal in living human cone photoreceptors. *Opt Express* 2010;18:5257–70.
- [15] LaVail MM, Yasumura D, Matthes M, Lau-Villacorta C, Unoki K, Sung C-H, et al. Protection of mouse photoreceptors by survival factors in retinal degenerations. *Invest Ophthalmol Vis Sci* 1998;39:592–602.
- [16] Lévillard T, Mohand-Said S, Lorentz O, Hicks D, Fintz A-C, Clérin E, et al. Identification and characterization of rod-derived cone viability factor. *Nat Genet* 2004;36(7):755–9.
- [17] Lévillard T, Sahel J-A. Rod-derived cone viability factor for treating blinding diseases: From clinic to redox signaling. *Sci Trans Med* 2010;2:1–13.
- [18] Longbottom R, Fruttigera M, Douglas RH, Martinez-Barberac JP, Greenwooda J, Mossa SE. Genetic ablation of retinal pigment epithelial cells reveals the adaptive response of the epithelium and impact on photoreceptors. *Proc Natl Acad Sci USA* 2009;3:18728–33.
- [19] Mohand-Said S, Hicks D, Lévillard T, Picaud S, Porto F, Sahel J-A. Rod-cone interactions: Developmental and clinical significance. *Prog Retin Eye Res* 2001;20(4):451–67.
- [20] O'Day W, Young R. Rhythmic daily shedding of outer-segment membranes by visual cells in the goldfish. *J Cell Biol* 1978;76:593–604.
- [21] Oyster CW. *The human eye: Structure and function*. Sinauer Associates, Inc.; 1999.
- [22] Papermaster DS. The birth and death of photoreceptors: The Friedenwald lecture. *Invest Ophthalmol Vis Sci* 2002;43(5):1300–4.
- [23] Phelan JK, Bok D. A brief review of retinitis pigmentosa and the identified retinitis pigmentosa genes. *Mol Vis* 2000;6:116–24.
- [24] Punzo C, Kornacker K, Cepko CL. Stimulation of the insulin/mTOR pathway delays cone death in a mouse model of retinitis pigmentosa. *Nat Neurosci* 2009;12(1):44–52.
- [25] Shintani K, Shechtman DL, Gurwood AS. Review and update: Current treatment trends for patients with retinitis pigmentosa. *Optometry* 2009;80:384–401.
- [26] van Soest S, Westerveld A, de Jong PTVM, Bleeker-Wagemakers EM, Bergen AAB. Retinitis pigmentosa: Defined from a molecular point of view. *Surv Ophthalmol* 1999;43:321–34.

- [27] Venkatesh A, Ma S, Le YZ, Hall MN, Rüegg MA, Punzo C. Activated mtorc1 promotes long-term cone survival in retinitis pigmentosa mice. *J Clin Invest* 2015;125:1446–58.
- [28] Wong F. Investigating retinitis pigmentosa: a laboratory scientist's perspective. *Prog Retin Eye Res* 1997;16:353–73.
- [29] Young RW. The renewal of rod and cone outer segments in the rhesus monkey. *J Cell Biol* 1971;49:303–18.
- [30] Young R. Visual cells and the concept of renewal. *Invest Ophthalmol Vis Sci* 1976;15:700–25.
- [31] Young RW, Bok D. Participation of the retinal pigment epithelium in the rod outer segment renewal process. *J Cell Biol* 1969;42:392–403.